

Traveling Wave Solutions to a Neural Field Model With Oscillatory Synaptic Coupling Types

Alan Dyson*

October 25, 2022

Abstract

In this paper, we investigate existence, uniqueness, and spectral stability of traveling waves arising from a single threshold neural field model with one spatial dimension, a Heaviside firing rate function, axonal propagation delay, and biologically motivated oscillatory coupling types. Since neuronal tracing studies show that long-ranged excitatory connections form stripe-like patterns throughout the mammalian cortex, we aim to generalize the notions of pure excitation, lateral inhibition, and lateral excitation by allowing coupling types to spatially oscillate between excitation and inhibition. In turn, we hope to analyze traveling fronts and pulses with novel shapes. With fronts as our main focus, we exploit Heaviside firing rate functions in order to establish existence and utilize speed index functions with at most one critical point as a tool for showing uniqueness of wave speed. Since fronts arising from Heaviside firing rate functions have closed-form solutions, we are able to easily construct Evans functions, the so-called stability index functions, in order to study spectral stability. Finally, we show that by incorporating slow linear feedback and moving to a system of integral differential equations, we can compute fast pulses numerically with phase space dynamics that are remarkably similar to their corresponding singular homoclinical orbits; hence, our work has connections to mathematical neuroscience as well as perturbation theory.

Key words. integral differential equations, traveling wave solutions, existence, stability, Evans function.

AMS subject classifications. 35B25, 92C20

1 Introduction

Modern research of the mammalian brain has significantly gravitated towards predicting, observing, and analysing traveling waves. The combination of using sophisticated electrode recording technology and pharmacologically blocking inhibition allows researchers to observe these patterns experimentally [22, 46]. Pathology and general physiological phenomenon are often strong motivators for such research; for example, traveling waves have been observed during epileptiform [5, 22, 46], migraines [33], and visual stimuli [1, 34, 45]. Naturally, computational and theoretical mathematical modeling arises in order to predict or explain propagations.

We gain insight as to why mathematical models have been proposed for decades by realizing that the mammalian nervous system is extraordinarily complex. For some perspective, comprehensive studies show that in a human neocortex, there are approximately 20 billion neurons and $.15 \times 10^{15}$ synapses [41]. Even a single synaptic event, spanning from an action potential

*Department of Mathematics, Lehigh University, 14 East Packer Avenue, Bethlehem, PA 18015 (acd313@lehigh.edu)

to neurotransmission, is highly nontrivial to model. Notably, the famous Hodgkin Huxley experiments [25] provided a basis for understanding the connection between action potentials and voltage-gated sodium and potassium channels. More models have been implemented in order to track the impact that neurotransmitters have on conductance after reaching their postsynaptic receptors. Changes caused by excitatory and inhibitory neurotransmitters lead to fast and slow dynamics based on receptor type [3]. By adding firing rate patterns such as oscillations and bursting [26] into the mix, we see that single neuron dynamics constitute a deep segment of neuroscience in their own right.

The difficulty level grows exponentially when we embed single cell dynamics into networks. After accounting for metabolic processes like spike frequency adaptation and synaptic depression at the network level, we may convince ourselves that macroscopic modeling has its place for capturing and predicting novel wave-like behaviors. While we acknowledge that there are different valid approaches to the problem, we choose to treat firing times of single neurons as uncorrelated [20] and consider a neural field model, treating space and time as continuous. Fittingly, we model firing rates as functions at the network level that only depend on the average voltage in spatial patches. Since average voltage is implicitly related to single neuron dynamics, we find that single neuron features are relevant, but significantly less emphasized.

Instead, our emphasis is on how patches of neurons connect based on spatial positioning. A key component of our model is invoking a homogeneous synaptic coupling weight kernel $K(x-y)$ to describe the spatial contribution to membrane potential that presynaptic neurons at position y contribute to postsynaptic neurons at position x . Here the sign of $K(x-y)$ determines whether the connection is inhibitory or excitatory and the magnitude determines the connection strength.

Coupling patterns in the neocortex described by oscillations of excitation and inhibition are known to exist and therefore, merit investigation. In particular, superficial layers such as layers 2 and 3 are where excitatory pyramidal cells make extensive arborizations laterally with inhibitory interneurons in the gaps [9]. Depending on the mammal and the brain region, tracing studies reveal excitatory stripes of varying patterns and purposes. For example, tracer injections in the visual cortex of cats reveal intercolumn connections are likely based on functional specificity [21]; intracortical connections are correlated with visual experiences [36] and context-dependent processing [39]. Similar horizontal connections have also been found in the primary visual cortexes of tree shrews [4] and macaque monkeys [37]. Experiments have also been carried on on the macaque monkey prefrontal cortex where biotinylated dextran amine was injected in the layer 3 prefrontal cortex of macaque monkeys and revealed long-range stripe-like connections [35, 37, 40].

Motivated by such biologically observed connection types, we seek traveling wave solutions arising from well-studied neural field models. Others have invoked similar coupling types in related work on traveling and standing waves arising from models like ours; see [2, 24, 30, 31, 32, 38, 50, 52].

1.1 Model Equations and Background

In this paper, fronts are our main focus. Thus, we study the following homogeneous neural field model with axonal transmission delay [12, 42]:

$$u_t + u = \alpha \int_{\mathbb{R}} K(x-y) H(u(y, t - \frac{1}{c_0}|x-y|) - \theta) dy, \quad (1.1)$$

where $u = u(x, t)$ is the mean electric potential in the spatial patch at position x and time t . The aforementioned kernel function K represents the coupling strength and type (excitatory or inhibitory) based on spatial positioning. The constant parameter $\alpha > 0$ controls synaptic coupling strength, while $\theta > 0$ is the single threshold of excitation for the network. A delay in transmission arises from the parameter c_0 , which is the speed of action potentials in the network. The Heaviside step function H represents the firing rate of a single neuron. In this simplified model, we can understand our firing rate function as a binary mechanism: if $u(x, t)$ is above a

threshold θ , the neurons in spatial patch x will fire at a maximum rate; otherwise, they will not fire at all. Such an assumption is used to simplify the analysis.

In order to understand the biophysical basis of (1.1), we briefly review the derivation in [12]. First suppose we have a fixed spatial patch of postsynaptic neurons x and N arbitrarily spaced presynaptic patches y_i for $i = 1, \dots, N$. Moreover, suppose we observe activity at times s_j for $j = 1, \dots, M$. For each i and j , activity from patch y_i at time s_j contributes

$$\alpha \eta(t - s_j) K(x - y_i) S(u(y_i, s_j - \frac{1}{c_0}|x - y_i|) \Delta y_i \Delta s_j$$

to the potential of neurons at patch x . Here $\eta(t - s)$ is the time dependent contribution that activity at time s has at time t , S is the firing rate for the network where axonal velocity delay is properly accounted for. Summing over all i and j , the total input to neurons at x is

$$\alpha \sum_{j=1}^M \sum_{i=1}^N \eta(t - s_j) K(x - y_i) S(u(y_i, s_j - \frac{1}{c_0}|x - y_i|) \Delta y_i \Delta s_j. \quad (1.2)$$

If we allow M and N to go to infinity and suppose (1.2) is the only input the neurons at x receive at time t , $u(x, t)$ takes on the form [12, 42]:

$$u(x, t) = \alpha \int_{-\infty}^t \eta(t - s) \int_{\mathbb{R}} K(x - y) S(u(y, s - \frac{1}{c_0}|x - y|) - \theta) dy ds. \quad (1.3)$$

Finally, for the special case where $\eta(t) = \exp(-t)H(t)$ and S is the Heaviside step function, differentiation of (1.3) leads to (1.1). Note that other choices for η may be implemented based on neurotransmitter dynamics.

Research concerning numerous wave form solutions of (1.1) has expanded largely because of some important initial results. Wilson and Cowan [47] were the first to study space and time coarse graining of local populations of interacting excitatory and inhibitory neurons. Amari was the first to obtain closed form standing wave solutions when a Heaviside firing rate function and Mexican hat kernel were used. In [12], Ermentrout and McLeod applied a homotopy argument to prove the existence of traveling fronts in the presence of sigmoidal firing rate functions and nonnegative kernels. For more background on the models, see [3, 6, 11, 13].

1.2 Main Goal and Improvement From Previous Results

In this paper, we are primarily concerned with proving the existence and uniqueness of traveling wave front solutions to (1.1) when the kernel $K(x)$ transversely intersects the x -axis at most countably many times. The resulting solutions $U(\cdot)$ are heteroclinical orbits that connect the fixed points $u \equiv 0$ and $u \equiv \alpha$, crossing the threshold θ exactly once. While this idea has been investigated before, we extend previous results.

Firstly, we expand the class of kernels such that (1.1) has traveling wave solutions with unique wave speeds. By translation invariance, we assume without loss of generality, that $U(0) = \theta$. In turn, we handle the unique wave speed problem using a speed index function, first derived by Pinto and Ermentrout [42] and later by others:

$$\phi(\mu) := \int_{-\infty}^0 \exp\left(\frac{c_0 - \mu}{c_0 \mu} x\right) K(x) dx. \quad (1.4)$$

Our main improvement can be seen in our handling of unique roots $\mu_0 \in (0, c_0)$ of the compatibility equation

$$\phi(\mu) = \frac{1}{2} - \frac{\theta}{\alpha}, \quad (1.5)$$

for $0 < 2\theta < \alpha$, arising from the requirement that the traveling waves cross the threshold exactly once. Under our methods, we consider three new biologically motivated types of oscillatory

kernel classes. The first class can be understood as an extension and combination of the analysis given by Zhang and Hutt [51] and Lijun Zhang, Linghai Zhang, Yuan, and Khaliq [52], Lv and Wang [38]. The other two class types are new; they are constructed with the intent of using the first derivative test on ϕ to show that ϕ has at most one critical point.

Secondly, we formulate the eigenvalue problem and examine spectral stability of our solutions for kernels of all three types. For the point spectrum, our main tool is the complex analytic Evans function [14, 15, 16, 17], the so-called stability index function, where roots are equivalent to eigenvalues. Although many authors have used the Evans function successfully, stability of traveling waves has not been discussed concerning many of the kernels considered in this paper. Originally derived by Zhang [48], we use the same Evans function as others have for our model – namely, by translation invariance of the front,

$$\mathcal{E}(\lambda) := 1 - \frac{\phi\left(\frac{\mu_0}{\lambda+1}\right)}{\phi(\mu_0)}, \quad (1.6)$$

with domain

$$\Omega = \{\lambda \in \mathbb{C} \mid \operatorname{Re}(\lambda) > -1\}.$$

We must show that $\mathcal{E}(\lambda)$ has no roots on the right half plane except for an algebraically simple root at $\lambda = 0$. For new kernels mentioned in this paper, the task appears to be analytically challenging. After we prove uniqueness of wave speed, we show that $\lambda = 0$ is a simple eigenvalue and that there are no real eigenvalues. Using surface plots of $|\mathcal{E}(\lambda)|$, we show that several examples of previously unstudied kernels lead to spectral stability.

We conclude with Section 5, where we motivate future work by computing fast traveling pulses arising from the singularly perturbed system of integral equations [42, 43]:

$$u_t + u + w = \alpha \int_{\mathbb{R}} K(x-y) H\left(u(y, t - \frac{1}{c_0}|x-y|) - \theta\right) dy, \quad (1.7)$$

$$w_t = \epsilon(u - \gamma w), \quad (1.8)$$

for $0 < \epsilon \ll 1$. Using the same example kernels used for the fronts, pulses are plotted and compared to singular solutions in phase space portraits.

In the proceeding two subsections, we sketch out our techniques for existence, uniqueness, and stability of fronts. In the sections thereafter, we develop the necessary rigor for our arguments.

1.3 Existence and Uniqueness of Wave Fronts Sketch

Our main result, accomplished in Section 3, is the following theorem when K is in one of the kernel classes formulated in Section 2.3.

Theorem 1.1 (Existence and Uniqueness of Front). *Suppose that $0 < 2\theta < \alpha$ and K is in class $\mathcal{A}_{j,k}$, $\mathcal{B}_{j,k}$, or $\mathcal{C}_{j,k}$ for some integers j and k . Then there exists a unique traveling wave front solution $u(x, t) = U(z)$ to (1.1) such that $U(0) = \theta$, $U'(0) > 0$, $U(z) < \theta$ on $(-\infty, 0)$, and $U(z) > \theta$ on $(0, \infty)$. The front satisfies the reduced equation*

$$\mu_0 U' + U = \alpha \int_{\mathbb{R}} K(z-y) H\left(U\left(y - \frac{\mu_0}{c_0}|z-y|\right) - \theta\right) dy \quad (1.9)$$

with exponentially decaying limits

$$\lim_{z \rightarrow -\infty} U(z) = 0, \quad \lim_{z \rightarrow \infty} U(z) = \alpha, \quad \lim_{z \rightarrow \pm\infty} U'(z) = 0.$$

The wave travels under the traveling coordinate $z = x + \mu_0 t$ at the unique wave speed $\mu_0 \in (0, c_0)$.

Accomplished in Section 3, we break down the proof of this theorem into three main steps.

1. The first step is to show how to transform (1.1) into a more palatable form and obtain a formal solution under the heuristic that one exists.

2. The second step is to use the condition $U(0) = \theta$ to obtain a unique wave speed μ_0 by locating unique solutions to (1.5).
3. The third and final step is to show the formal solution really is a traveling wave in the sense that the formal solution really does only cross the threshold one time.

After we prove existence and uniqueness of the traveling wave fronts, we explore the spectral stability of our solutions.

1.4 Spectral Stability Sketch

Our main method is linearization. We first change x to the traveling coordinate z and write (1.1) as

$$P_t + \mu_0 P_z + P = \alpha \int_{\mathbb{R}} K(z-y) H\left(P(y - \frac{\mu_0}{c_0}|z-y|, t - \frac{1}{c_0}|z-y|) - \theta\right) dy. \quad (1.10)$$

Letting $p(z, t) = P(z, t) - U(z)$ and linearizing (1.10) about the wave front, we yield

$$p_t + \mu_0 p_z + p = \frac{\alpha c_0}{U'(0)(c_0 + \text{sgn}(z)\mu_0)} K\left(\frac{c_0}{c_0 + \text{sgn}(z)\mu_0} z\right) p\left(0, t - \frac{|z|}{c_0 + \text{sgn}(z)\mu_0}\right). \quad (1.11)$$

Setting $p(z, t) = \exp(\lambda t)\psi(z)$, we produce a nonlinear eigenvalue problem $\mathcal{L}(\lambda)\psi = \lambda\psi$, where the family of operators $\mathcal{L}(\lambda) : C^1(\mathbb{R}) \cap L^\infty(\mathbb{R}) \rightarrow C^0(\mathbb{R}) \cap L^\infty(\mathbb{R})$ are defined by

$$\begin{aligned} \mathcal{L}(\lambda)\psi = & -\mu_0\psi' - \psi + \frac{\alpha c_0}{U'(0)(c_0 + \text{sgn}(z)\mu_0)} K\left(\frac{c_0}{c_0 + \text{sgn}(z)\mu_0} z\right) \\ & \times \exp\left(-\frac{\lambda|z|}{c_0 + \text{sgn}(z)\mu_0}\right)\psi(0). \end{aligned} \quad (1.12)$$

Using standard notation, we denote $\sigma(\mathcal{L})$ to be the spectrum of \mathcal{L} , which is made up of the point spectrum and essential spectrum; the point spectrum is made up of eigenvalues. We establish the following important definition.

Definition 1.1. A traveling wave solution to (1.1) is *spectrally stable* if the following conditions hold:

- (i) The essential spectrum $\sigma_{\text{essential}}(\mathcal{L})$ lies entirely to the left of the imaginary axis.
- (ii) There exists a positive constant $\kappa_0 > 0$ such that $\max\{\text{Re } \lambda \mid \lambda \in \sigma_{\text{point}}(\mathcal{L}), \lambda \neq 0\} \leq -\kappa_0$.
- (iii) The eigenvalue $\lambda = 0$ is algebraically simple.

In Section 4, we discuss techniques for achieving (ii) and (iii) using the celebrated Evans function [14, 15, 16, 17]. In particular, we use Zhang's [48] closed-form derivation of the Evans function for neuronal networks with Heaviside firing rate functions. In related work, many other authors have used the Evans function approach; see [7, 18, 23, 43, 51]. We are now ready to construct the biologically motivated kernels that are the focal point of this paper.

2 Kernel Constructions

In this section, we systematically describe the oscillatory kernel classes we wish to study; examples are then provided in Section 2.3.

Basic Assumptions and Terminology

In all cases, we assume our kernel K has the following typical properties for this type of problem:

$$\int_{-\infty}^0 K(x) dx = \int_0^{\infty} K(x) dx = \frac{1}{2}, \quad |K(x)| \leq C \exp(-\rho|x|) \quad \text{for all } x \in \mathbb{R}.$$

For some background, we define commonly used kernel types that oscillate at most once on each half plane.

Definition 2.1. We say K is a *pure excitation* kernel if $K(x) \geq 0$ for all x .

Definition 2.2. We say K is a *lateral inhibition* kernel, or Mexican hat kernel, if there exists unique constants $M_1 > 0$ and $M_2 > 0$ such that $K(x) \geq 0$ on $(-M_1, M_2)$ and $K(x) \leq 0$ on $(-\infty, -M_1) \cup (M_2, \infty)$.

Definition 2.3. We say K is a *lateral excitation* kernel, or upside down Mexican hat kernel, if there exists unique constants $N_1 > 0$ and $N_2 > 0$ such that $K(x) \geq 0$ on $(-\infty, -N_1) \cup (N_2, \infty)$ and $K(x) \leq 0$ on $(-N_1, N_2)$.

We will come back to these definitions in Section 2.4 after we have defined our oscillatory kernel classes.

2.1 Existence and Uniqueness of Wave Speed

The conditions presented in this subsection, which we shall call *wave speed conditions*, underlie the most substantial difference between this work and others. This subsection provides the groundwork for obtaining the existence and uniqueness of wave speeds when the kernel functions oscillate any number of times on the left half plane. The following repeated integral of $|x|K(x)$, originally proposed in [51], will be used throughout the paper:

$$\begin{aligned}\Lambda^0 K(x) &:= |x|K(x), \\ \Lambda^n K(x) &:= \int_x^0 \int_{x_{n-1}}^0 \dots \int_{x_1}^0 |x_0|K(x_0) dx_0 \dots dx_{n-2} dx_{n-1} \\ &= \int_x^0 \Lambda^{n-1} K(x_{n-1}) dx_{n-1} \quad \text{for } x \leq 0 \text{ and } n \geq 1.\end{aligned}\tag{2.1}$$

Using this definition, we define three wave speed conditions.

- (A_n) Suppose there exists $n \geq 0$ such that $\Lambda^n K(x) \geq 0$ for all $x \leq 0$. Then we say K satisfies wave speed condition (A_n).
- (B_n) Suppose there exists $n \geq 0$ and a constant $B_n > 0$ such that $\Lambda^n K(x) \geq 0$ on $(-B_n, 0)$ and $\Lambda^n K(x) \leq 0$ on $(-\infty, -B_n)$. Then we say K satisfies wave speed condition (B_n).
- (C_n) Suppose there exists $n \geq 0$ and a constant $C_n > 0$ such that $\Lambda^n K(x) \leq 0$ on $(-C_n, 0)$ and $\Lambda^n K(x) \geq 0$ on $(-\infty, -C_n)$. Then we say K satisfies wave speed condition (C_n).

We now preview the following lemma, which will be proved in Section 3.2, in order to motivate the distinct strategies behind each wave speed condition. Part (i) was proven in [51] using wave speed condition (A_n).

Lemma 3.1 (Unique Wave Speed).

- (i) Suppose K satisfies wave speed condition (A_n) for some $n \geq 0$ and all other assumptions hold. Then $\phi'(\mu) > 0$ for all $\mu \in (0, c_0)$. Thus, there exists a unique solution $\mu_0 \in (0, c_0)$ to (1.5).
- (ii) Suppose K satisfies wave speed condition (B_n) for some $n \geq 0$ and all other assumptions hold. Then ϕ has at most one critical point, a local maximum, guaranteed to exist if $\int_{-\infty}^0 |x|K(x) dx < 0$. Such a local maximum occurs when $\phi > \frac{1}{2}$ and thus, there exists a unique solution $\mu_0 \in (0, c_0)$ to (1.5).
- (iii) Suppose K satisfies wave speed condition (C_n) for some $n \geq 0$ and all other assumptions hold. Then ϕ has at most one critical point, a local minimum, guaranteed to exist if $K(0) < 0$. Such a local minimum occurs when $\phi < 0$ and thus, there exists a unique solution $\mu_0 \in (0, c_0)$ to (1.5).

Following the outline in Section 1.3, we now establish left and right half plane conditions used to complete Step 3.

2.2 Conditions to Ensure Wave Front Threshold Requirements

The preceding left and right half plane conditions, which we will call *threshold conditions*, ensure that regardless of how much K oscillates, our traveling wave front solution satisfies $U(\cdot) < \theta$ on $(-\infty, 0)$ and $U(\cdot) > \theta$ on $(0, \infty)$.

Left Half Plane Threshold Conditions

We consider situations where K transversely crosses the negative x -axis at most countably many times. The first preceding condition \mathcal{L}_0 represents pure excitation on the left half plane. The next condition \mathcal{L}_j was formulated from the original work in [52, Assumptions $(L_2) - (L_3)$, p. 2-3]. We do, however, remove the requirements

$$\int_{-M_{2n}}^{-M_{2n-2}} |x|K(x) dx \geq 0, \quad \int_{-M_{2n}}^0 |x|K(x) dx \geq 0 \quad (2.2)$$

for $1 \leq n < \infty$, since these estimates are special cases of wave speed condition (A_1) .

Based on the methods in [52], the requirements in (2.2) appear to be the main barrier that prevents their kernel classes from including kernels that oscillate infinitely many times. By modifying these requirements, we overcome this obstacle. We see such improvement in the creation of condition \mathcal{L}_∞ below. Furthermore, we present the conditions \mathcal{L}_{-j} and $\mathcal{L}_{-\infty}$, which for $j \neq 1$ are new and arise since we may use wave speed condition (C_n) .

\mathcal{L}_0 : Suppose $K(x) \geq 0$ on $(-\infty, 0)$. Then K satisfies condition \mathcal{L}_0 .

\mathcal{L}_j : Suppose K transversely crosses the negative x -axis exactly j times in the sense that there exists constants $0 < M_1 < M_2 < \dots < M_j$ such that $K(-M_n) = 0$ and $\text{sgn}(K'(-M_n)) = (-1)^{n+1}$ for $n = 1, 2, \dots, j$. Also, if $j \geq 2$, suppose

$$\frac{\alpha}{2} - \alpha \int_{-M_{2n}}^0 K(x) dx < \theta \quad \text{for } n = 1, 2, \dots, \left\lfloor \frac{j}{2} \right\rfloor.$$

Then K satisfies condition \mathcal{L}_j . If K transversely crosses the negative x -axis infinitely many times, we allow $j \rightarrow \infty$.

\mathcal{L}_{-j} : Suppose K transversely crosses the negative x -axis exactly j times in the sense that there exists constants $0 < M_1 < \dots < M_j$ such that $K(-M_n) = 0$ and $\text{sgn}(K'(-M_n)) = (-1)^n$ for $n = 1, 2, \dots, j$. Also, if $j \geq 3$, suppose

$$\frac{\alpha}{2} - \alpha \int_{-M_{2n+1}}^0 K(x) dx < \theta \quad \text{for } n = 1, 2, \dots, \left\lfloor \frac{j-1}{2} \right\rfloor.$$

Then K satisfies condition \mathcal{L}_{-j} . If K transversely crosses the negative x -axis infinitely many times, we allow $j \rightarrow \infty$.

The main physical difference between \mathcal{L}_j and \mathcal{L}_{-j} can be understood in the following manner: For a fixed postsynaptic patch of neurons x , the local presynaptic neurons y satisfying $x < y < x + M_1$ will be excitatory if $K(x - y)$ satisfies \mathcal{L}_j and inhibitory if $K(x - y)$ satisfies \mathcal{L}_{-j} . A similar physical interpretation can be drawn from \mathcal{R}_k and \mathcal{R}_{-k} below, but with the position of local presynaptic neurons relative to x reversed.

Right Half Plane Threshold Conditions

Conditions \mathcal{R}_k and \mathcal{R}_{-k} below come directly from [52, Assumption $(R_2) - (R_6)$, p. 3]. However, we allow K to oscillate infinitely many times on the right half plane, as seen by conditions \mathcal{R}_∞ and $\mathcal{R}_{-\infty}$ respectively.

\mathcal{R}_0 Suppose $K(x) \geq 0$ on $(0, \infty)$. Then K satisfies condition \mathcal{R}_0 .

\mathcal{R}_k : Suppose K transversely crosses the positive x -axis exactly k times in the sense that there exists constants $0 < N_1 < \dots < N_k$ such that $K(N_n) = 0$ and $\text{sgn}(K'(N_n)) = (-1)^n$ for $n = 1, 2, \dots, k$. Also, if $k \geq 2$, suppose

$$\frac{\alpha}{2} + \alpha \int_0^{N_{2n}} K(x) dx > \theta \quad \text{for } n = 1, \dots, \left\lfloor \frac{k}{2} \right\rfloor.$$

Then K satisfies condition \mathcal{R}_k . If K transversely crosses the positive x -axis infinitely many times, we allow $k \rightarrow \infty$.

\mathcal{R}_{-k} : Suppose K transversely crosses the positive x -axis exactly k times in the sense that there exists constants $0 < N_1 < \dots < N_k$ such that $K(N_n) = 0$ and $\text{sgn}(K'(N_n)) = (-1)^{n+1}$ for $n = 1, \dots, k$. Also, suppose

$$\frac{\alpha}{2} + \alpha \int_0^{N_{2n-1}} K(x) dx > \theta \quad \text{for } n = 1, \dots, \left\lfloor \frac{k+1}{2} \right\rfloor.$$

Then K satisfies condition \mathcal{R}_{-k} . If K transversely crosses the positive x -axis infinitely many times, we allow $k \rightarrow \infty$.

Remark 2.1. If K is symmetric, as it often is assumed to be for these types of problems, and satisfies \mathcal{L}_j for $j \geq 1$, then K also satisfies \mathcal{R}_k for $k = j$.

2.3 Three Families of Kernel Classes

We define the following types of kernel classes used throughout this paper:

$\mathcal{A}_{j,k}$ Suppose on the left half plane, K satisfies threshold condition \mathcal{L}_j for some $j \geq 0$ and wave speed condition (A_n) for some $n \geq 0$; on the right half plane K satisfies threshold condition \mathcal{R}_k for some $k \geq 0$. Then we say K is in class $\mathcal{A}_{j,k}$.

$\mathcal{B}_{j,k}$ Suppose on the left half plane, K satisfies threshold condition \mathcal{L}_j for some $j \geq 1$ and wave speed condition (B_n) for some $n \geq 0$; on the right half plane K satisfies threshold condition \mathcal{R}_k for some $k \geq 0$. Then we say K is in class $\mathcal{B}_{j,k}$.

$\mathcal{C}_{j,k}$ Suppose on the left half plane, K satisfies threshold condition \mathcal{L}_{-j} for some $j \geq 1$ and wave speed condition (C_n) for some $n \geq 0$; on the right half plane K satisfies threshold condition \mathcal{R}_{-k} for some $k \geq 0$. Then we say K is in class $\mathcal{C}_{j,k}$.

We recall that $K(x - y)$ means the spatial impact that neurons located at position y contribute to neurons located at position x . Therefore, by simply knowing the kernel class under the framework above, we can instantly acquire intuition as to how excitatory and inhibitory contributions are modulated to the left and right of a fixed position x .

Remark 2.2. In rare circumstances such as when $\int_{-\infty}^0 |x|K(x) dx = 0$ or $K(0) = 0$, a kernel may fit the definition of multiple kernel classes, which we see as inconsequential.

Examples

Before we proceed with proving our results, we consider three examples of kernels that oscillate countably many times. These kernels will be used throughout the paper to supplement our understanding of how the kernel classes connect to existence, uniqueness, and stability of wave front solutions to (1.1). We also use the same example kernels when studying the pulse in Section 5. In all cases, the kernels are symmetric and normalized by a constant A in order to integrate to one. The rest of the model parameters are assigned the values $\alpha = 1$, $\theta = 0.4$, and $c_0 = 1$.

Example 2.1. The first example is a kernel in class $\mathcal{A}_{\infty, \infty}$:

$$K_1(x) := A \exp(-a|x|)(\cos(bx) + c), \quad (2.3)$$

where $a = 0.2$, $b = 2$, $c = 0.4$.

Example 2.2. The second example is a kernel in class $\mathcal{B}_{\infty,\infty}$:

$$K_2(x) := A \exp(-a|x|)(a \sin(|x|) + \cos(x)), \quad (2.4)$$

where $a = 0.3$. This type of kernel has already been studied explicitly in the setting of standing waves in [10, 30, 32] and traveling waves in [8, 10].

Example 2.3. The third example is a kernel in class $\mathcal{C}_{\infty,\infty}$:

$$K_3(x) := A \exp(-a|x|)(\cos(bx) - c), \quad (2.5)$$

where $a = 0.2$, $b = 2$, $c = 0.4$.

In Figures 1, 2, and 3, we may visually verify that K_1 and K_2 satisfy threshold conditions \mathcal{L}_{∞} and \mathcal{R}_{∞} , while K_3 satisfies threshold conditions $\mathcal{L}_{-\infty}$ and $\mathcal{R}_{-\infty}$.

Not pictured: kernels K_1 , K_2 , and K_3 satisfy wave speed conditions (A_2) , (B_2) , and (C_1) respectively.

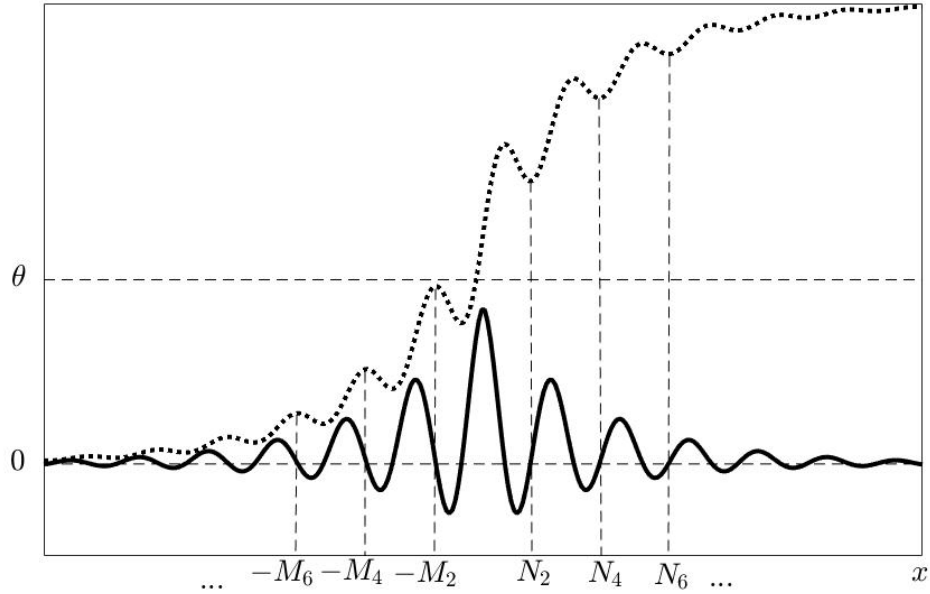


Figure 1: Plot of $K_1(x)$ (solid) and $\frac{\alpha}{2} - \alpha \int_x^0 K_1(y) dy$ (dotted).

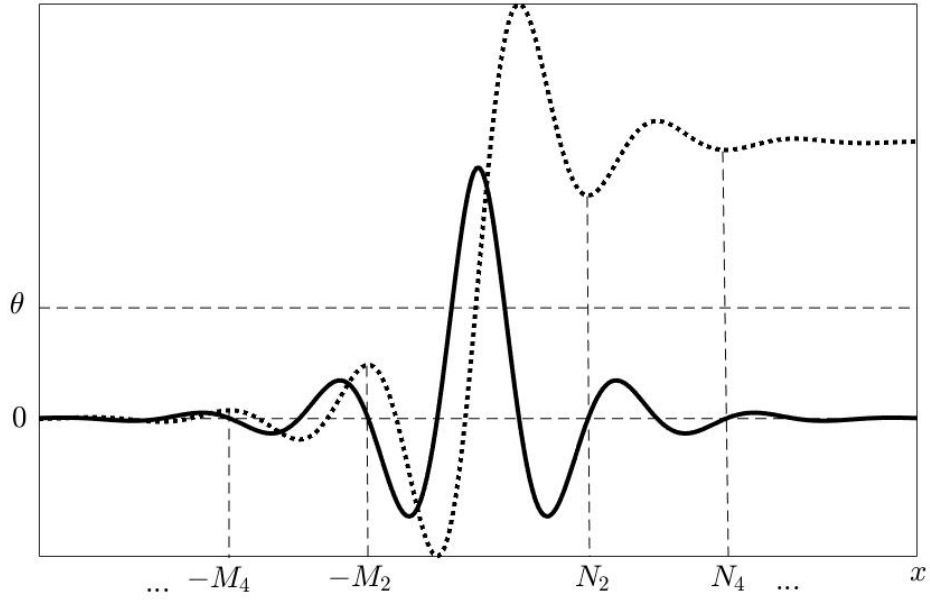


Figure 2: Plot of $K_2(x)$ (solid) and $\frac{\alpha}{2} - \alpha \int_x^0 K_2(y) dy$ (dotted).

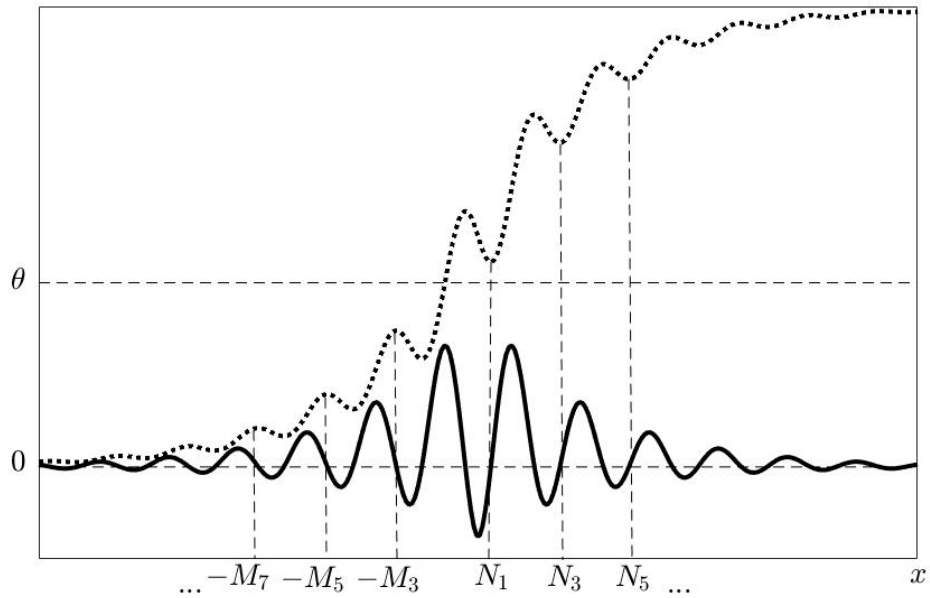


Figure 3: Plot of $K_3(x)$ (solid) and $\frac{\alpha}{2} - \alpha \int_x^0 K_3(y) dy$ (dotted).

2.4 Results From Previous Kernels

Other authors have studied kernels that oscillate at most finitely many times on the left and right half planes respectively. In the case of zero oscillations, existence, uniqueness, and stability of traveling wave solutions to (1.1) and similar models arising from pure excitation kernels (seen as class $\mathcal{A}_{0,0}$) have been studied in tremendous depth; the resulting traveling wave solutions are monotonic with Evans functions that are easy to handle. The analysis immediately becomes more challenging when K may oscillate on the left and right half planes even once as a lateral inhibition or lateral excitation kernel.

In such circumstances, Zhang [49] studied the existence, uniqueness, and stability of traveling wave solutions to (1.1). For lateral inhibition kernels, he imposed the condition $\int_{-\infty}^0 |x|K(x) dx \geq 0$ in order to guarantee uniqueness of wave speed. In this paper, such kernels can be regarded as lateral inhibition kernels that satisfy the wave speed condition (A_1) and are therefore in class $\mathcal{A}_{1,1}$. The consideration that $\int_{-\infty}^0 |x|K(x) dx < 0$ is necessarily the case where K is in class $\mathcal{B}_{1,1}$, which has not been studied before. Hence, our results complete the existence and uniqueness of traveling wave solutions to (1.1) arising from all exponentially bounded lateral inhibition kernels. Similarly, by noting that lateral excitation kernels are in class $\mathcal{C}_{1,1}$, we see that classes $\mathcal{A}_{j,k}$, $\mathcal{B}_{j,k}$ and $\mathcal{C}_{j,k}$ include and generalize lateral inhibition and lateral excitation kernels.

Beyond lateral inhibition and lateral excitation kernels, others have explored kernels with more oscillations. Notably, Lv and Wang [38] first created five oscillatory kernel classes and proved the existence and uniqueness of the corresponding front solutions to (1.1). Although their methods are important, all of their kernels cross the x -axis at most four times. Using similar techniques and kernel assumptions, Zhang et al. [52] and Lijun Zhang [50] improved their results by increasing the maximum number of oscillations to any finite number.

However, the main limitations in [38, 50, 52] arise from the kernel assumptions they employ to guarantee the fronts have unique wave speeds. In particular, for kernels with more than one oscillation on the left half plane, they do not allow their speed index functions to have any critical points. Rather than using the repeated integral function $\Lambda^n K(x)$ and wave speed conditions from Section 2.1, they impose stronger conditions. In the most nonrestrictive cases, their kernels satisfy condition (A_n) in the special case where $n = 1$. Moreover, conditions (B_n) and (C_n) are not discussed at all.

Such limitations have a some notable consequences. One consequence is that they were unable to study kernels that oscillated countably many times. Another important consequence is that although their kernel classes include lateral excitation kernels, they were unable to consider classes $\mathcal{C}_{j,k}$ for $j > 1$. From a biological perspective, this means that oscillatory kernels modeling local inhibition were largely neglected.

On the other end of the spectrum, in a more general model, Zhang and Hutt [51, Subsection 2.3, parts d1,d2 p. 32-34] considered the unique wave speed problem for kernels that oscillated finitely or infinitely many times. However, they only studied the threshold requirements of fronts corresponding with pure excitation, lateral inhibition, and lateral excitation kernels. They point out and prove that if a kernel that oscillates finitely or countably many times satisfies wave speed condition (A_n) for some $n \geq 1$, then the speed index function is strictly increasing. However, they also did not invoke conditions (B_n) and (C_n) , preventing them from studying speed index functions with single critical points.

Elvin et al. [10] studied the existence, uniqueness, and stability of fronts arising from the kernel type given in Example 2.2. However, their approach was ad hoc with a heavy emphasis on bifurcation analysis.

3 Analysis of Front Existence

In this section, our goal is to rigorously prove Theorem 1.1. Specifically, we analyse all three necessary steps outlined in Section 1.3.

3.1 Step 1: Formal solution

Starting with the original scalar equation (1.1), we let $z = x + \mu_0 t$ and $u(x, t) = U(z)$. Equation (1.1) immediately reduces to

$$\mu_0 U' + U = \alpha \int_{\mathbb{R}} K(z - y) H \left(U \left(y - \frac{\mu_0}{c_0} |z - y| \right) - \theta \right) dy. \quad (3.1)$$

Under the change of variable $\eta = y - \frac{\mu_0}{c_0} |z - y|$, we have $z - y = \frac{c_0}{c_0 + \text{sgn}(z - \eta)\mu_0} (z - \eta)$ and $dy = \frac{c_0}{c_0 + \text{sgn}(z - \eta)\mu_0} d\eta$. Using the assumption $U(\cdot) > \theta$ on $(0, \infty)$ and $U(\cdot) < \theta$ on $(-\infty, 0)$, we arrive at the equation

$$\begin{aligned} \mu_0 U' + U &= \alpha \int_0^\infty \frac{c_0}{c_0 + \text{sgn}(z - \eta)\mu_0} K \left(\frac{c_0}{c_0 + \text{sgn}(z - \eta)\mu_0} (z - \eta) \right) d\eta \\ &= \alpha \int_{-\infty}^{\frac{c_0 z}{c_0 + \text{sgn}(z)\mu_0}} K(x) dx. \end{aligned} \quad (3.2)$$

Keeping the boundary conditions in mind, equation (3.2) can easily be easily solved using variation of parameters. After solving and simplifying with integration by parts, we obtain the solution representation

$$\begin{aligned} U(z) &= \alpha \int_{-\infty}^{\frac{c_0 z}{c_0 + \text{sgn}(z)\mu_0}} K(x) dx \\ &\quad - \alpha \int_{-\infty}^z \frac{c_0}{c_0 + \text{sgn}(x)\mu_0} \exp \left(\frac{x - z}{\mu_0} \right) K \left(\frac{c_0 x}{c_0 + \text{sgn}(x)\mu_0} \right) dx, \end{aligned} \quad (3.3)$$

$$U'(z) = \frac{\alpha}{\mu_0} \int_{-\infty}^z \frac{c_0}{c_0 + \text{sgn}(x)\mu_0} \exp \left(\frac{x - z}{\mu_0} \right) K \left(\frac{c_0 x}{c_0 + \text{sgn}(x)\mu_0} \right) dx. \quad (3.4)$$

3.2 Step 2: Existence and Uniqueness of Traveling Wave Speed

Existence

Setting $U(0) = \theta$, as deemed necessary by Theorem 1.1, we see that if $\mu_0 \in (0, c_0)$ exists and is unique, it must be the only solution to the equation

$$\phi(\mu) = \frac{1}{2} - \frac{\theta}{\alpha}, \quad (1.5)$$

where we recall from the introduction,

$$\phi(\mu) := \int_{-\infty}^0 \exp \left(\frac{c_0 - \mu}{c_0 \mu} x \right) K(x) dx \quad (1.4)$$

is the speed index function. Since the integrand of ϕ is exponentially bounded, we use dominated convergence theorem and see that

$$\lim_{\mu \rightarrow 0^+} \phi(\mu) = 0, \quad \lim_{\mu \rightarrow c_0^-} \phi(\mu) = \int_{-\infty}^0 K(x) dx = \frac{1}{2}.$$

Finally, since $0 < \frac{1}{2} - \frac{\theta}{\alpha} < \frac{1}{2}$ by assumption, we use the intermediate value theorem to conclude there exists at least one solution to (1.5). The main difficulty is utilizing the assumptions on the kernel to prove uniqueness.

Uniqueness

In this subsection, we prove Lemma 3.1. Part (i) was first proven in [51, Subsection 2.3, parts d1,d2 p. 32-34]¹ for a similar model.

Lemma 3.1 (Unique Wave Speed).

- (i) Suppose K satisfies wave speed condition (A_n) for some $n \geq 0$ and all other assumptions hold. Then $\phi'(\mu) > 0$ for all $\mu \in (0, c_0)$. Thus, there exists a unique solution $\mu_0 \in (0, c_0)$ to (1.5).
- (ii) Suppose K satisfies wave speed condition (B_n) for some $n \geq 0$ and all other assumptions hold. Then ϕ has at most one critical point, a local maximum, guaranteed to exist if $\int_{-\infty}^0 |x|K(x) dx < 0$. Such a local maximum occurs when $\phi > \frac{1}{2}$ and thus, there exists a unique solution $\mu_0 \in (0, c_0)$ to (1.5).
- (iii) Suppose K satisfies wave speed condition (C_n) for some $n \geq 0$ and all other assumptions hold. Then ϕ has at most one critical point, a local minimum, guaranteed to exist if $K(0) < 0$. Such a local minimum occurs when $\phi < 0$ and thus, there exists a unique solution $\mu_0 \in (0, c_0)$ to (1.5).

Proof. (i) Differentiating ϕ and using integration by parts n times, we may write

$$\begin{aligned}
\phi'(\mu) &= \frac{1}{\mu^2} \int_{-\infty}^0 |x| \exp\left(\frac{c_0 - \mu}{c_0 \mu} x\right) K(x) dx \\
&= \frac{1}{\mu^2} \int_{-\infty}^0 \exp\left(\frac{c_0 - \mu}{c_0 \mu} x\right) \Lambda^0 K(x) dx \\
&= \frac{1}{\mu^2} \int_{-\infty}^0 \exp\left(\frac{c_0 - \mu}{c_0 \mu} x\right) \left[-\Lambda^1 K(x)\right]' dx \\
&= \frac{c_0 - \mu}{c_0 \mu} \frac{1}{\mu^2} \int_{-\infty}^0 \exp\left(\frac{c_0 - \mu}{c_0 \mu} x\right) \Lambda^1 K(x) dx \\
&\vdots \\
&= \left(\frac{c_0 - \mu}{c_0 \mu}\right)^n \frac{1}{\mu^2} \int_{-\infty}^0 \exp\left(\frac{c_0 - \mu}{c_0 \mu} x\right) \Lambda^n K(x) dx.
\end{aligned} \tag{3.5}$$

Since K satisfies wave speed condition (A_n) , we have $\Lambda^n K(x) \geq 0$ for $x \leq 0$. Therefore, $\phi'(\mu) > 0$ for all $\mu \in (0, c_0)$ so there exists a unique solution $\mu_0 \in (0, c_0)$ to (1.5).

(ii) For all n , define the function

$$\zeta_n(\mu) := \int_{-\infty}^0 \exp\left(\frac{c_0 - \mu}{c_0 \mu} x\right) \Lambda^n K(x) dx. \tag{3.6}$$

We observe that the sign of ϕ' and ζ_n are equivalent since $\mu < c_0$ and by (3.5),

$$\phi'(\mu) = \left(\frac{c_0 - \mu}{c_0 \mu}\right)^n \frac{1}{\mu^2} \zeta_n(\mu). \tag{3.7}$$

Since K satisfies wave speed condition (B_n) , there exists a constant $B_n > 0$ such that $\Lambda^n K(x) \geq 0$ on $(-B_n, 0)$ and $\Lambda^n K(x) \leq 0$ on $(-\infty, -B_n)$. Suppose $\phi'(\mu_*) = 0$ for some

¹An inconsequential error was made that is corrected here.

$\mu_* \in (0, c_0)$. This implies $\zeta_n(\mu_*) = 0$ and

$$\begin{aligned}
\zeta_n'(\mu_*) &= \frac{1}{\mu_*} \int_{-\infty}^0 |x| \exp\left(\frac{c_0 - \mu_*}{c_0 \mu_*} x\right) \Lambda^n K(x) dx \\
&= \frac{1}{\mu_*} \left[\int_{-B_n}^0 |x| \exp\left(\frac{c_0 - \mu_*}{c_0 \mu_*} x\right) \Lambda^n K(x) dx + \int_{-\infty}^{-B_n} |x| \exp\left(\frac{c_0 - \mu_*}{c_0 \mu_*} x\right) \Lambda^n K(x) dx \right] \\
&< \frac{B_n}{\mu_*} \left[\int_{-B_n}^0 \exp\left(\frac{c_0 - \mu_*}{c_0 \mu_*} x\right) \Lambda^n K(x) dx + \int_{-\infty}^{-B_n} \exp\left(\frac{c_0 - \mu_*}{c_0 \mu_*} x\right) \Lambda^n K(x) dx \right] \\
&= \frac{B_n}{\mu_*} \zeta_n(\mu_*) \\
&= 0.
\end{aligned}$$

Hence, $\zeta_n(\mu)$ changes signs from positive to negative at $\mu = \mu_*$. Since ζ_n and ϕ' have equivalent signs, we may conclude that ϕ has a local maximum at $\mu = \mu_*$ by the first derivative test. Moreover, since μ_* is arbitrary and ϕ is differentiable on $(0, c_0)$, we conclude that all critical points of ϕ must be local maximums. Finally, we have

$$\lim_{\mu \rightarrow 0^+} \phi(\mu) = 0, \quad \lim_{\mu \rightarrow c_0^-} \phi(\mu) = \frac{1}{2}, \quad \lim_{\mu \rightarrow c_0^-} \phi'(\mu) = \frac{1}{c_0^2} \int_{-\infty}^0 |x| K(x) dx \quad (3.8)$$

so if $\int_{-\infty}^0 |x| K(x) dx < 0$, such a μ_* will exist by the intermediate value theorem and $\phi(\mu_*) > \frac{1}{2}$. Therefore, ϕ is strictly increasing when $0 < \phi < \frac{1}{2}$ so there exists a unique solution $\mu_0 \in (0, c_0)$ to (1.5).

- (iii) We proceed similarly to (ii). Since K satisfies wave speed condition (C_n) , there exists a constant $C_n > 0$ such that $\Lambda^n K(x) \leq 0$ on $(-C_n, 0)$ and $\Lambda^n K(x) \geq 0$ on $(-\infty, -C_n)$. Suppose $\phi'(\mu_*) = 0$ for some $\mu_* \in (0, c_0)$. Then as before, $\zeta_n(\mu_*) = 0$ and

$$\begin{aligned}
\zeta_n'(\mu_*) &= \frac{1}{\mu_*} \int_{-\infty}^0 |x| \exp\left(\frac{c_0 - \mu_*}{c_0 \mu_*} x\right) \Lambda^n K(x) dx \\
&= \frac{1}{\mu_*} \left[\int_{-C_n}^0 |x| \exp\left(\frac{c_0 - \mu_*}{c_0 \mu_*} x\right) \Lambda^n K(x) dx + \int_{-\infty}^{-C_n} |x| \exp\left(\frac{c_0 - \mu_*}{c_0 \mu_*} x\right) \Lambda^n K(x) dx \right] \\
&> \frac{C_n}{\mu_*} \left[\int_{-C_n}^0 \exp\left(\frac{c_0 - \mu_*}{c_0 \mu_*} x\right) \Lambda^n K(x) dx + \int_{-\infty}^{-C_n} \exp\left(\frac{c_0 - \mu_*}{c_0 \mu_*} x\right) \Lambda^n K(x) dx \right] \\
&= \frac{C_n}{\mu_*} \zeta_n(\mu_*) \\
&= 0.
\end{aligned}$$

We apply the first derivative test on ϕ again; this time we find that ϕ has a local minimum at $\mu = \mu_*$ and conclude that critical points of ϕ must be local minimums. By a change of variable, we may write

$$\phi'(\mu) = \int_{-\infty}^0 |x| \exp\left(\frac{c_0 - \mu}{c_0} x\right) K(\mu x) dx.$$

A trivial calculation shows that the sign of $\phi'(0)$ is determined by the sign of $K(0)$. Finally, since K satisfies wave speed condition (C_n) , it follows that $K(0) \leq 0$; if $K(0) < 0$, such a local minimum will exist with $\phi(\mu_*) < 0$. Therefore, by similar reasoning to (ii), ϕ is strictly increasing when $0 < \phi < \frac{1}{2}$ so there exists a unique solution $\mu_0 \in (0, c_0)$ to (1.5). \square

See Figure 4. As a corollary to Lemma 3.1, we may easily answer an open problem: does a front solution to (1.1) arising from a lateral inhibition kernel with $\int_{-\infty}^0 |x|K(x) dx < 0$ have a unique wave speed?

Corollary 3.1. *Suppose K is any lateral inhibition kernel. Then there exists a unique solution $\mu_0 \in (0, c_0)$ to (1.5) independent of the value of $\int_{-\infty}^0 |x|K(x) dx$.*

Proof. Independent of $\int_{-\infty}^0 |x|K(x) dx$, K satisfies wave speed condition (B_0) . Applying Lemma 3.1 (ii), the result follows. \square

Combining the results of Step 1 with Lemma 3.1, we see that if our formal solutions are in fact real fronts, they will have unique wave speeds. The last step we must take is proving that the solutions satisfy the necessary threshold requirements to be actual solutions. After this step, our proof of existence and uniqueness of front solutions to (1.1) will be complete.

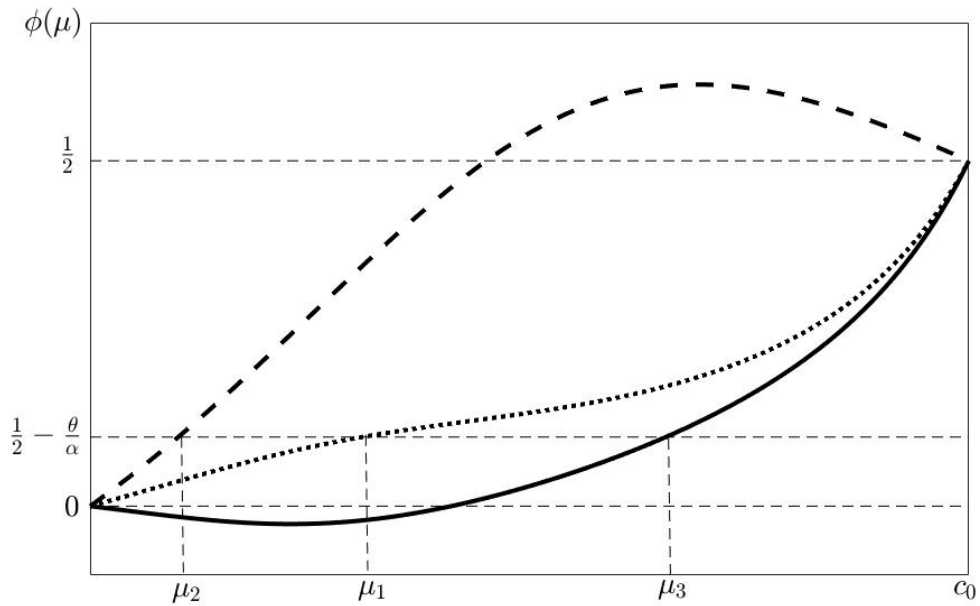


Figure 4: Plots of $\phi(\mu)$ for kernels K_1 (dotted), K_2 (dashed), and K_3 (solid).

3.3 Step 3: Formal Solution is a Real Solution

The main intent of this step is to use the threshold conditions outlined in Section 2.2 to prove that $U(0) = \theta$, $U(z) < \theta$ on $(-\infty, 0)$, and $U(z) > \theta$ on $(0, \infty)$. We analyse the left and right half planes separately.

Following the original approach by Lv and Wang [38] and generalized by Lijun Zhang [50], Zhang et al. [52], our technique is to show that on the left half plane, our conditions on K are sufficient in guaranteeing that all possible local maximums of U lie below the threshold. On the right half plane, we show that all possible local minimums of U lie above the threshold.

We now prove the following lemmas using a modified version of [52, Lemma 3 and 4, p. 6]. The modifications account for the case where K oscillates infinitely many times and when K satisfies \mathcal{L}_{-j} for $j > 1$.

Lemma 3.2. *If K satisfies \mathcal{L}_j or \mathcal{L}_{-j} for some $j \geq 0$, then $U(z) < \theta$ on $(-\infty, 0)$.*

Proof. If K satisfies \mathcal{L}_j for some $0 \leq j < \infty$, see [52, Lemma 4, p. 6]. The case where $j = \infty$ is a trivial extension of the same argument: since $\alpha \int_{-\infty}^0 K(x) dx = \frac{\alpha}{2}$, there exists a positive integer $N(\alpha, \theta)$ such that $\frac{\alpha}{2} - \alpha \int_{-M_{2n}}^0 K(x) dx < \theta$ for all $n \geq N(\alpha, \theta)$. Hence, the argument for the $0 \leq j < \infty$ case can be applied again.

If K satisfies \mathcal{L}_{-j} for some $j \geq 1$, we adjust the argument in [52]. For $z \leq 0$, define

$$\begin{aligned} \psi(z) &:= \int_{-\infty}^z \exp\left(\frac{c_0 - \mu_0}{c_0 \mu_0} x\right) K(x) dx \\ &= \left(\frac{1}{2} - \frac{\theta}{\alpha}\right) - \int_z^0 \exp\left(\frac{c_0 - \mu_0}{c_0 \mu_0} x\right) K(x) dx. \end{aligned} \quad (3.9)$$

The sign of $U'\left(\frac{c_0 - \mu_0}{c_0} z\right)$ is determined by $\psi(z)$ since

$$\begin{aligned} U'\left(\frac{c_0 - \mu_0}{c_0} z\right) &= \frac{\alpha}{\mu_0} \exp\left(-\frac{c_0 - \mu_0}{c_0 \mu_0} z\right) \int_{-\infty}^z \exp\left(\frac{c_0 - \mu_0}{c_0 \mu_0} x\right) K(x) dx \\ &= \frac{\alpha}{\mu_0} \exp\left(-\frac{c_0 - \mu_0}{c_0 \mu_0} z\right) \psi(z). \end{aligned} \quad (3.10)$$

If $j = 1$, then $\psi(z)$ is increasing on $(-\infty, -M_1)$, decreasing on $(-M_1, 0)$ with $\psi(0) = \frac{1}{2} - \frac{\theta}{\alpha} > 0$ and $\lim_{z \rightarrow -\infty} \psi(z) = 0$. Therefore, $\psi(z) \geq 0$ on $(-\infty, 0)$ so $U(z)$ is monotonic on $(-\infty, 0)$.

If $j = 2$, then $\psi(z)$ is decreasing on $(-\infty, -M_2) \cup (-M_1, 0)$, increasing on $(-M_2, -M_1)$. Since $\psi(0) > 0$ and $\lim_{z \rightarrow -\infty} \psi(z) = 0$, we conclude that $\psi(z)$ changes signs exactly one time, from negative to positive for some $z_* \in (-M_2, -M_1)$. But this mean $U(z)$ has a local minimum at $z = \frac{c_0 - \mu_0}{c_0} z_*$ and no local maximums on $(-\infty, 0)$.

If $j \geq 3$, then $\psi(z)$ is increasing on $(-M_{2n+2}, -M_{2n+1})$ and decreasing on $(-M_{2n+1}, -M_{2n})$ for $n \geq 0$, where we let $M_0 = 0$. Based again on the fact that $\psi(0) > 0$ and $\lim_{z \rightarrow -\infty} \psi(z) = 0$, we see that if $\psi(z)$ changes signs from positive to negative at $z = z_*$, and therefore $U(z)$ has a local maximum at $z = \frac{c_0 - \mu_0}{c_0} z_*$, then $z_* \in (-M_{2n+1}, -M_{2n})$ for $n \geq 1$. But then

$$\begin{aligned} U\left(\frac{c_0 - \mu_0}{c_0} z_*\right) &= \alpha \int_{-\infty}^{z_*} K(x) dx - \mu_0 U'\left(\frac{c_0 - \mu_0}{c_0} z_*\right) \\ &= \alpha \int_{-\infty}^{z_*} K(x) dx \\ &= \frac{\alpha}{2} - \alpha \int_{z_*}^0 K(x) dx \\ &< \frac{\alpha}{2} - \alpha \int_{-M_{2n+1}}^0 K(x) dx \\ &< \theta. \end{aligned} \quad (3.11)$$

Therefore, U stays below the threshold on all possible local maximums. \square

Lemma 3.3. *If K satisfies \mathcal{R}_k or \mathcal{R}_{-k} for some $k \geq 0$, then $U(z) > \theta$ on $(0, \infty)$.*

Proof. If $k < \infty$, see [52]. The extension to the $k \rightarrow \infty$ case is similar to the $j \rightarrow \infty$ case in Lemma 3.2. \square

3.4 Summary of Existence and Uniqueness

Let us recall the main result, that is:

Theorem 1.1 (Existence and Uniqueness of Front). *Suppose that $0 < 2\theta < \alpha$ and K is in class $\mathcal{A}_{j,k}$, $\mathcal{B}_{j,k}$, or $\mathcal{C}_{j,k}$ for some integers j and k . Then there exists a unique traveling wave front solution $u(x,t) = U(z)$ to (1.1) such that $U(0) = \theta$, $U'(0) > 0$, $U(z) < \theta$ on $(-\infty, 0)$, and $U(z) > \theta$ on $(0, \infty)$. The front satisfies the reduced equation*

$$\mu_0 U' + U = \alpha \int_{\mathbb{R}} K(z-y) H\left(U\left(y - \frac{\mu_0}{c_0}|z-y|\right) - \theta\right) dy \quad (1.9)$$

with exponentially decaying limits

$$\lim_{z \rightarrow -\infty} U(z) = 0, \quad \lim_{z \rightarrow \infty} U(z) = \alpha, \quad \lim_{z \rightarrow \pm\infty} U'(z) = 0.$$

The wave travels under the traveling coordinate $z = x + \mu_0 t$ at the unique wave speed $\mu_0 \in (0, c_0)$.

Proof. Combining Lemmas 3.1 to 3.3, the result follows. \square

Corollary 3.2. *Suppose that $0 < 2\theta < \alpha$ and K is any lateral inhibition kernel. Then independent of the value of $\int_{-\infty}^0 |x|K(x) dx$, there exists a unique traveling wave front to (1.1) as described by Theorem 1.1.*

Proof. For lateral inhibition kernels, it is well known (see [49]) that the argument for existence of at least one front solution to (1.1) is independent of the value of $\int_{-\infty}^0 |x|K(x) dx$. By Corollary 3.1, uniqueness of wave speed is established. \square

See Figure 5 for plots of $U(z)$ with kernels K_1 , K_2 , and K_3 .

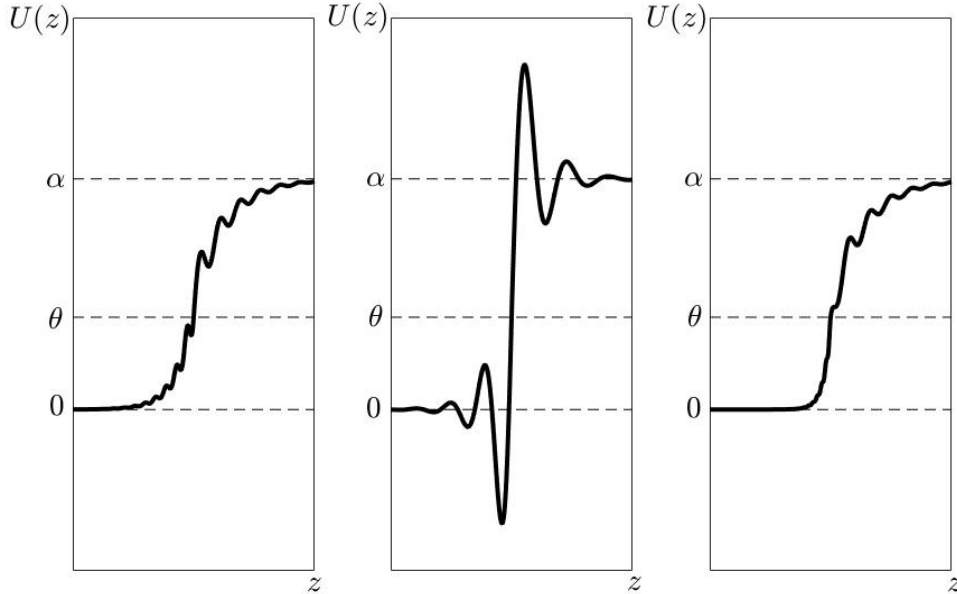


Figure 5: Plots of $U(z)$ for kernels K_1 (left), K_2 (center), and K_3 (right).

A natural concern is whether the solutions satisfy any criteria for stability. We have shown that a physiologically motivated model permits traveling wave solutions. However, actual neuronal networks are surely more complex than our model. Hence, in order for our analysis to be biologically useful, our solutions must ideally persist under the influence of small perturbations.

We now build off of the sketch in Section 1.4 and derive the Evans function in order to discuss spectral stability of our fronts.

4 Spectral Stability

Motivated by the pioneering work of Evans [14, 15, 16, 17] on the Hodgkin-Huxley model and Jones [28] on the Fitzhugh-Nagumo model, stability of traveling wave solutions has also been well developed for nonlocal equations. In particular, Zhang [48] studied spectral stability of (5.1)-(5.2) in the case where $c_0 = \infty$ (no delay); he formulated a closed form Evans function and used it to solve the linear eigenvalue problem. The problem came full circle when Sandstede [44] proved that in appropriate function spaces, spectral stability implies nonlinear stability. Interestingly, when there is delay, a rigorous proof of a similar connection has not been given and is still an open problem. The main difficulty is the fact that the eigenvalue problem becomes nonlinear in λ .

Some partial results have been made: Zhang [49] studied the spectral stability of wave front solutions to (1.1) arising from pure excitation, lateral inhibition, and lateral excitation kernels. Coombes and Owen [7] analysed and discussed the spectral stability in a more general setting (such as in (1.3)) using similar techniques to Zhang. The proceeding discussion is aimed at applying their techniques and leaving the reader with some open problems.

Recalling Section 1.4, we wish to solve the nonlinear eigenvalue problem $\mathcal{L}(\lambda)\psi = \lambda\psi$ where the family of linear operators $\mathcal{L}(\lambda) : C^1(\mathbb{R}) \cap L^\infty(\mathbb{R}) \rightarrow C^0(\mathbb{R}) \cap L^\infty(\mathbb{R})$ are defined by

$$\begin{aligned} \mathcal{L}(\lambda)\psi := & -\mu_0\psi' - \psi + \frac{\alpha c_0}{U'(0)(c_0 + \operatorname{sgn}(z)\mu_0)} K\left(\frac{c_0 z}{c_0 + \operatorname{sgn}(z)\mu_0}\right) \\ & \times \exp\left(-\frac{\lambda|z|}{c_0 + \operatorname{sgn}(z)\mu_0}\right)\psi(\lambda, 0). \end{aligned} \quad (1.12)$$

The essential spectrum of $\mathcal{L}(\lambda)$ is easily determined by the intermediate eigenvalue problem $\mathcal{L}^\infty\psi = \lambda\psi$, where

$$\mathcal{L}^\infty\psi := -\mu_0\psi' - \psi, \quad (4.1)$$

which is linear in ψ and λ . A trivial calculation shows the intermediate eigenvalue problem is solved by

$$\psi_0(\lambda, z) = C(\lambda) \exp\left(-\frac{\lambda+1}{\mu_0}z\right). \quad (4.2)$$

Assuming $C(\lambda) \neq 0$, the solution $\psi_0(\lambda, z)$ blows up as $z \rightarrow -\infty$ when $\operatorname{Re}(\lambda) > -1$ and as $z \rightarrow \infty$ when $\operatorname{Re}(\lambda) < -1$. Thus, the essential spectrum is the vertical line

$$\sigma_{\text{essential}} = \{\lambda \in \mathbb{C} \mid \operatorname{Re}(\lambda) = -1\}, \quad (4.3)$$

which safely stays entirely on the left half plane. Hence, on the domain

$$\Omega = \{\lambda \in \mathbb{C} \mid \operatorname{Re}(\lambda) > -1\},$$

the stability is determined by σ_{point} , which notably depends on K . Through a series of calculations [7, 49], the eigenvalue problem is solved by

$$\begin{aligned} \psi(\lambda, z) = & C(\lambda) \exp\left(-\frac{\lambda+1}{\mu_0}z\right) + \frac{\alpha\psi(\lambda, 0)}{\mu_0 U'(0)} \int_{-\infty}^z \frac{c_0}{c_0 + \operatorname{sgn}(x)\mu_0} \exp\left(\frac{\lambda+1}{\mu_0}(x-z)\right) \\ & \times \exp\left(-\frac{\lambda|x|}{c_0 + \operatorname{sgn}(x)\mu_0}\right) K\left(\frac{c_0 x}{c_0 + \operatorname{sgn}(x)\mu_0}\right) dx. \end{aligned} \quad (4.4)$$

Since $\psi(\lambda, 0)$ appears on the right hand side in (4.4), we must plug in $z = 0$ and solve for $C(\lambda)$ to ensure ψ is well-defined. For $\lambda \in \Omega$, nontrivial solutions $\psi(\lambda, z)$ do not blow up as $z \rightarrow \pm\infty$ if and only if $C(\lambda) = 0$. We obtain an Evans function whose zeros entirely determine σ_{point} . By translation invariance, $\lambda = 0$ is an eigenvalue with eigenfunction $U'(z)$. Hence, the Evan's function, written in terms of the speed index function ϕ , is given explicitly by

$$\mathcal{E}(\lambda) := 1 - \frac{\phi\left(\frac{\mu_0}{\lambda+1}\right)}{\phi(\mu_0)}. \quad (1.6)$$

Since the elegant formulation of \mathcal{E} is not a new result, we present the following lemma without proof. See [48] for the details.

Lemma 4.1.

- (i) *The Evans function is complex analytic on Ω and real if λ is real.*
- (ii) *The complex number $\lambda_0 \in \sigma_{point}$ if and only if $\mathcal{E}(\lambda_0) = 0$.*
- (iii) *The algebraic multiplicity of eigenvalues of $\mathcal{L}(\lambda)$ is exactly equal to the multiplicity of zeros of $\mathcal{E}(\lambda)$.*
- (iv) *In the domain Ω , the Evans function has the asymptotic behavior $\lim_{|\lambda| \rightarrow \infty} \mathcal{E}(\lambda) = 1$.*

Recalling the criteria for spectral stability given in Section 1.4, a traveling wave front is spectrally stable if there does not exist any eigenvalues with $\text{Re}(\lambda) \geq 0$, except for $\lambda = 0$, which must be a simple eigenvalue.

We already know $\lambda = 0$ is an eigenvalue of multiplicity at least one. Moreover,

$$\mathcal{E}'(\lambda) = \frac{\mu_0}{(\lambda + 1)^2} \frac{\phi'(\frac{\mu_0}{\lambda+1})}{\phi(\mu_0)}, \quad (4.5)$$

which implies $\mathcal{E}'(0) = \mu_0 \frac{\phi'(\mu_0)}{\phi(\mu_0)} > 0$ for all K in classes $\mathcal{A}_{j,k}$, $\mathcal{B}_{j,k}$, and $\mathcal{C}_{j,k}$. By Lemma 4.1 (iii), it follows that $\lambda = 0$ is a simple eigenvalue.

We now consider the behavior of $\mathcal{E}(\lambda)$ for λ on the positive real axis. For such λ , by uniqueness of the wave speed, $\phi(\frac{\mu_0}{\lambda+1}) \neq \phi(\mu_0)$. Therefore, $\mathcal{E}(\lambda) \neq 0$ so λ cannot be an eigenvalue.

We are finally brought to the difficult part of the stability analysis: if any, where are the zeros of $\mathcal{E}(\lambda)$ when $\text{Re}(\lambda) \geq 0$ and $\text{Im}(\lambda) \neq 0$? For most of the kernels discussed in this paper, this question appears to be nontrivial. As evident by the plots in Figure 6, we see that for at least some of our kernels, even the ones that oscillate countably many times, we have spectral stability of our wave fronts. However, it is currently unclear how often instability occurs, if at all. An avenue for further research would be to either prove outright or develop a reasonably nonrestrictive criteria to guarantee stability. If counterexamples can be given, are there any defining features of the kernels that lead to instability?

We close this section by pointing out that since \mathcal{E} is complex analytic, there are a number of options at our disposal. By Lemma 4.1 (iv) and the fact that zeros of \mathcal{E} must be isolated, the number of zeros on the right half plane is a finite number and contained in the region

$$B_{\delta,R} = \{\lambda \in \Omega \mid \text{Re}(\lambda) \geq 0 \text{ and } \delta \leq |\lambda| \leq R\}$$

for some $R \gg 0$, $\delta > 0$. Common tools like maximum principle or argument principle can be applied.

For example, it is certainly true that $|1 - \mathcal{E}(\lambda)| < 1$ when $|\lambda| = R$. If we can show $|1 - \mathcal{E}(\lambda)| < 1$ along the imaginary axis when $\delta \leq |\lambda| \leq R$, then $|1 - \mathcal{E}(\lambda)| < 1$ on $B_{\delta,R}$ by the maximum principle. Hence $|\mathcal{E}(\lambda)| > 0$ on $B_{\delta,R}$ and stability follows.

Finally, when specific kernels are given, we can use mathematical software to look at real and imaginary contour plots of $\mathcal{E}(\lambda)$ (as was done in [7]) or surface plots of $|\mathcal{E}(\lambda)|$ on the right half plane. In the examples given in Figure 6, we have chosen the latter option.

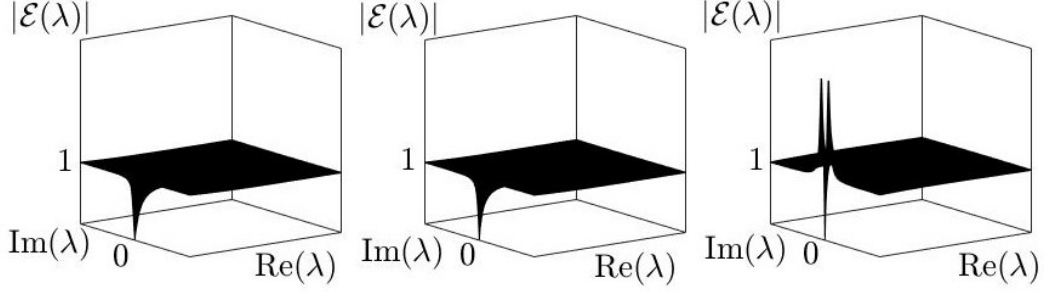


Figure 6: Surface plot of $|\mathcal{E}(\lambda)|$ with kernels K_1 (left), K_2 , (center), and K_3 (right) when $\text{Re}(\lambda) \geq 0$. In all cases, $|\mathcal{E}(\lambda)| > 0$ except at $\lambda = 0$, showing spectral stability.

5 Existence of Traveling Pulses

With some exceptions, traveling wave fronts alone are typically not that biologically interesting since they unrealistically ignore metabolic processes that generate negative feedback. Their main value comes from their close connection with traveling pulses; studying the existence and stability of the front is the preparation for studying the existence and stability of pulses. Since the methodology is more unclear for multiple pulses, we will only focus on single pulses.

Mathematically, pulses can be categorized as slow or fast based on the wave speed. Slow pulses are unstable perturbations of standing pulses, while fast stable pulses have a singular structure partially comprised of stable fronts and backs. For simplicity, we will ignore slow pulses since they are biologically less important.

Incorporating linear feedback into (1.1), we obtain the following system of integral equations [42, 43]:

$$u_t + u + w = \alpha \int_{\mathbb{R}} K(x-y) H(u(y, t - \frac{1}{c_0}|x-y|) - \theta) dy, \quad (5.1)$$

$$w_t = \epsilon(u - \gamma w), \quad (5.2)$$

where w is a slow leaking current and $0 < \epsilon \ll 1$ is a perturbation parameter. Biologically, w represents phenomenon like spike frequency adaptation.

By a fast pulse solution to (5.1)-(5.2), we mean a solution $(u, w) = (U_{pulse}(z), W_{pulse}(z))$ such that there exists a constant $\mathcal{Z}(\epsilon) > 0$ such that $U_{pulse}(0) = U_{pulse}(\mathcal{Z}(\epsilon)) = \theta$, $U_{pulse}(z) > \theta$ on $(0, \mathcal{Z}(\epsilon))$, $U_{pulse}(z) < \theta$ on $(-\infty, 0) \cup (\mathcal{Z}(\epsilon), \infty)$, and $\lim_{z \rightarrow \pm\infty} (U_{pulse}(z), W_{pulse}(z)) = (0, 0)$.

Here, $z = x + \mu(\epsilon)t$ is the traveling coordinate with unique fast wave speed $\mu(\epsilon) = \mu_{front} + \kappa(\epsilon)$, where $\kappa(\epsilon) \rightarrow 0$ as $\epsilon \rightarrow 0$.

Since the system is singularly perturbed, we cannot simply set $\epsilon = 0$ and obtain a solution that reasonably approximates a pulse. However, we can construct singular homoclinical orbits in phase space and argue that for $0 < \epsilon \ll 1$, real pulses are close to singular pulses. Such a singular homoclinical orbit is comprised of a front, back, and two space curves. The front and back (which have the same wave speed) are understood to capture the fast dynamics, while the two space curves are where slow time dynamics occur. Naturally, as pointed out in [42], the subject of geometric singular perturbation theory may be a method for proving pulses exist. However, working out the details is quite nontrivial since (5.1)-(5.2) is not necessarily

autonomous; applying geometric singular perturbation theory rigorously to (5.1)-(5.2) is still an open problem for general kernel functions.

We remark that many kernels presented in this paper (as evident by the examples given) allow us to convert (5.1)-(5.2) into a system of real, nonlinear, autonomous PDEs. The dynamics then reside in a more familiar setting to possibly apply techniques like the celebrated Exchange Lemma [27, 29] in the setting of center-stable and center-unstable manifold theory. The main setback in our problem is that the Heaviside firing rate function creates phase space dynamics with discontinuities; it is important that this issue is properly dealt with in order to apply such a technical result. Some promising partial results have been obtained in [18, 19] for related models with smooth firing rate functions.

Pulses have also been proven to exist using more direct computational tools like implicit function theorem, as was done in [43] when $K(x) = \frac{\rho}{2} \exp(-\rho|x|)$. Although this is a powerful result, the exact structure of K played an important role. Again, it is not entirely clear how to rigorously prove the existence of pulses to (5.1)-(5.2) for general kernel functions.

Numerically Computed Fast Pulses

In this subsection, we first derive formulas for fast pulses formally and then calculate pulses with example kernels K_1, K_2 , and K_3 respectively. Using phase space plots, we show that our solutions are real pulses. To simplify the discussion, we assume $c_0 = \infty$.

We wish to find traveling pulse solutions to (5.1)-(5.2) when $0 < 2\theta < \alpha < \frac{(1+\gamma)\theta}{\gamma}$, $0 < \epsilon \ll 1$ and K is a kernel such that a unique front is produced when $\epsilon = 0$. Assuming a pulse exists with $\mu(\epsilon)$ and $\mathcal{Z}(\epsilon)$ to be determined, (5.1)-(5.2) reduces to

$$\mu(\epsilon)U' + U + W = \alpha \int_{z-\mathcal{Z}(\epsilon)}^z K(x) dx, \quad (5.3)$$

$$\mu(\epsilon)W' = \epsilon(U - \gamma W), \quad (5.4)$$

which is easily solved using elementary techniques. The solution takes on the form

$$U_{pulse}(z) = \frac{\alpha\gamma}{1+\gamma} \int_{z-\mathcal{Z}(\epsilon)}^z K(x) dx - \alpha \int_{-\infty}^z C(x-z, \mu(\epsilon), \epsilon) [K(x) - K(x-\mathcal{Z}(\epsilon))] dx, \quad (5.5)$$

$$U'_{pulse}(z) = \alpha \int_{-\infty}^z C_x(x-z, \mu(\epsilon), \epsilon) [K(x) - K(x-\mathcal{Z}(\epsilon))] dx \quad (5.6)$$

$$W_{pulse}(z) = \frac{\alpha}{1+\gamma} \int_{z-\mathcal{Z}(\epsilon)}^z K(x) dx - \epsilon\alpha \int_{-\infty}^z D(x-z, \mu(\epsilon), \epsilon) [K(x) - K(x-\mathcal{Z}(\epsilon))] dx, \quad (5.7)$$

where

$$C(x, \mu(\epsilon), \epsilon) = \frac{1}{\omega_1(\epsilon) - \omega_2(\epsilon)} \left[\frac{1 - \omega_2(\epsilon)}{\omega_1(\epsilon)} \exp\left(\frac{\omega_1(\epsilon)}{\mu(\epsilon)}x\right) - \frac{1 - \omega_1(\epsilon)}{\omega_2(\epsilon)} \exp\left(\frac{\omega_2(\epsilon)}{\mu(\epsilon)}x\right) \right],$$

$$D(x, \mu(\epsilon), \epsilon) = \frac{1}{\omega_1(\epsilon) - \omega_2(\epsilon)} \left[-\frac{1}{\omega_1(\epsilon)} \exp\left(\frac{\omega_1(\epsilon)}{\mu(\epsilon)}x\right) + \frac{1}{\omega_2(\epsilon)} \exp\left(\frac{\omega_2(\epsilon)}{\mu(\epsilon)}x\right) \right],$$

$$\omega_1(\epsilon) = \frac{1 + \gamma\epsilon + \sqrt{(1 - \gamma\epsilon)^2 - 4\epsilon}}{2},$$

$$\omega_2(\epsilon) = \frac{1 + \gamma\epsilon - \sqrt{(1 - \gamma\epsilon)^2 - 4\epsilon}}{2}.$$

The parameters $\omega_1(\epsilon)$ and $\omega_2(\epsilon)$ are the eigenvalues associated with the coefficient matrix $A(\epsilon) = \begin{pmatrix} 1 & 1 \\ -\epsilon & \gamma\epsilon \end{pmatrix}$. We assume that ϵ and γ are sufficiently small so that both eigenvalues are positive.

Similar to the front, we must use the compatibility equations $U_{pulse}(0) = U_{pulse}(\mathcal{Z}(\epsilon)) = \theta$ to solve for $\mu(\epsilon)$ and $\mathcal{Z}(\epsilon)$, provided they exist. Then we must verify that the formal solutions lead to real traveling pulse solutions that satisfy the threshold requirements. As mentioned above, there are typically two solution pairs, $(\mu_{fast}(\epsilon), \mathcal{Z}_{fast}(\epsilon))$ and $(\mu_{slow}(\epsilon), \mathcal{Z}_{slow}(\epsilon))$, leading to stable and unstable pulses respectively [42, 43]. Since it is not entirely clear how to rigorously prove the existence of pulses for all kernels studied in this paper, we simply calculate $(\mu_{fast}(\epsilon), \mathcal{Z}_{fast}(\epsilon))$ numerically; then we compare the solutions to the singular solutions and argue that real fast pulses exist.

In Figures 7, 8, and 9, we see evidence that fast pulses exist for our kernel classes.

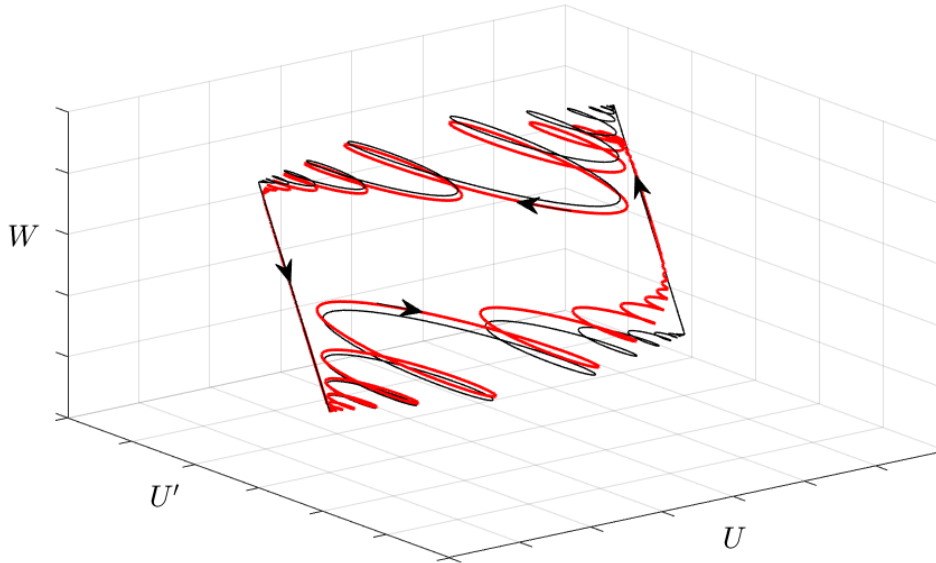


Figure 7: Red: Phase space portrait of a fast traveling pulse with kernel K_1 , $\alpha = 1$, $\theta = 0.4$, $\epsilon = \gamma = 0.001$. Black: Corresponding singular homoclinical orbit when $\epsilon = 0$.

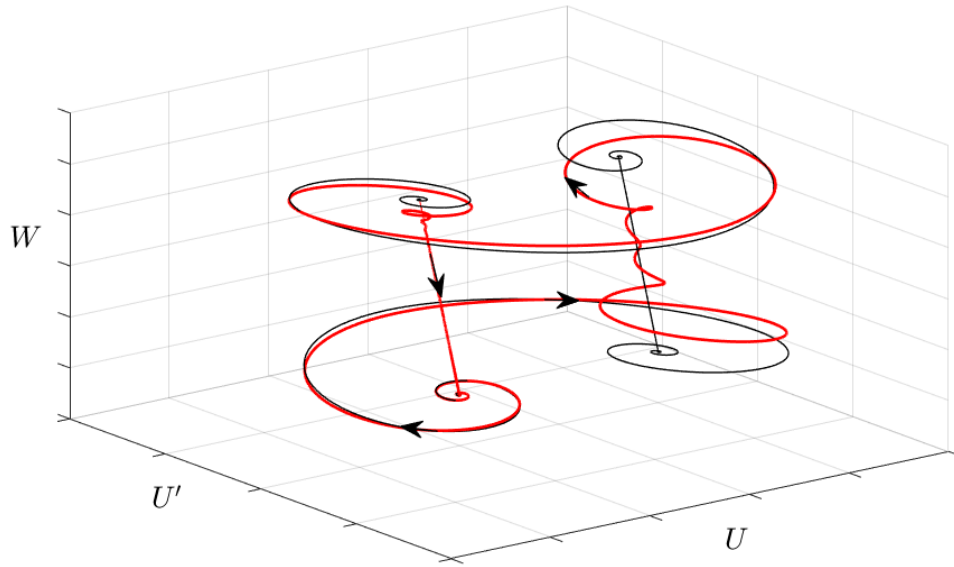


Figure 8: Red: Phase space portrait of a fast traveling pulse with kernel K_2 , $\alpha = 1$, $\theta = 0.4$, $\epsilon = \gamma = 0.001$. Black: Corresponding singular homoclinical orbit when $\epsilon = 0$.

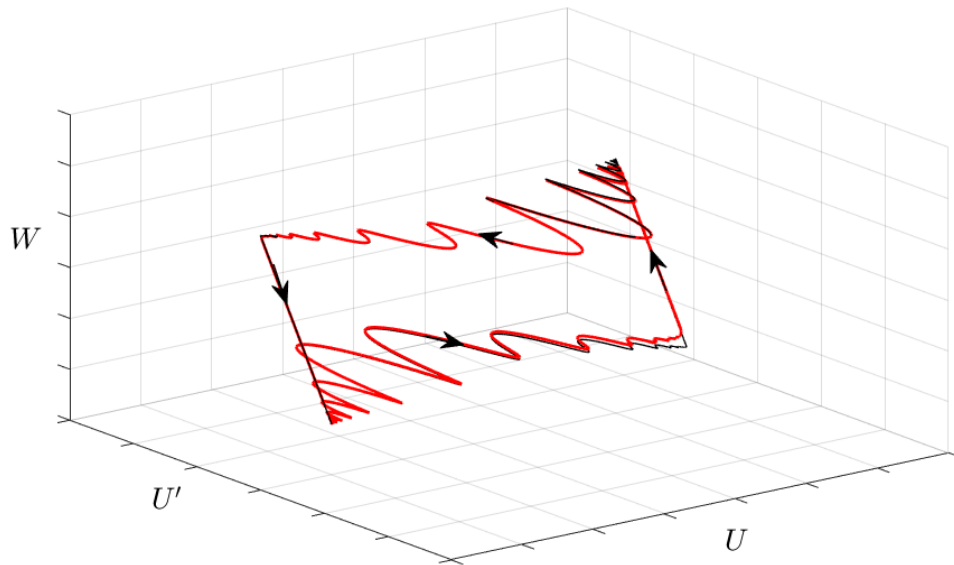


Figure 9: Red: Phase space portrait of a fast traveling pulse with kernel K_3 , $\alpha = 1$, $\theta = 0.4$, $\epsilon = \gamma = 0.001$. Black: Corresponding singular homoclinical orbit when $\epsilon = 0$.

Note that all plots were constructed in Matlab. For the fast pulses, the parameters $\mu(\epsilon)$ and $\mathcal{Z}(\epsilon)$ were computed using the Optimization Toolbox.

Discussion

In this paper, we proved the existence and uniqueness of traveling front solutions to (1.1) for a wide range of oscillatory kernel classes. To establish uniqueness, we chose the kernel classes in such a way that their corresponding speed index functions had at most one critical point. In order to make sure that the fronts crossed the threshold exactly once, we established left and right half plane conditions, following the techniques in [38, 50, 52].

In Section 4, we studied the spectral stability of our fronts using a standard method: linearizing the original equation and deriving an Evans function. Using three examples of kernels that oscillated countably many times, we plotted the Evans functions and showed that in all three examples, the fronts were spectrally stable. This demonstration has inspired some interesting open problems: How many of our kernel classes lead to stable versus unstable fronts? Can a meaningful bifurcation criteria be formulated?

Lastly, in Section 5, we reviewed the connection between fronts and fast pulses that arise in singularly perturbed integral differential equations. We derived pulses formally and numerically calculated fast pulses for all three example kernels used throughout the paper. Phase space portraits show that indeed, fast pulses are small perturbations of singular homoclinical orbits when $0 < \epsilon \ll 1$. Similar to Section 4, we desire a rigorous technique for proving the existence and uniqueness of fast pulses when K crosses the x -axis at most countably many times. How often do fast pulses exist for kernels in this paper? Can we obtain fronts for smoothed Heaviside firing rate functions? If so, we may be able to apply typical methods from perturbation theory.

Acknowledgements

The author would like to acknowledge his advisor, Linghai Zhang, for his guidance as well as valuable suggestions and criticisms of this paper.

References

- [1] A. BENUCCI, R. A. FRAZOR, AND M. CARANDINI, *Standing waves and traveling waves distinguish two circuits in visual cortex*, *Neuron*, 55 (2007), pp. 103–117.
- [2] F. BOTELHO, J. JAMISON, AND A. MURDOCK, *Single-pulse solutions for oscillatory coupling functions in neural networks*, *J. Dynam. Differential Equations*, 20 (2008), pp. 165–199.
- [3] P. C. BRESSLOFF, *Waves in neural media*, *Lect. Notes Math. Model. Life Sci.*, (2014), pp. 271–318.
- [4] H. J. CHISUM, F. MOOSER, AND D. FITZPATRICK, *Emergent properties of layer 2/3 neurons reflect the collinear arrangement of horizontal connections in tree shrew visual cortex*, *J. Neurosci.*, 23 (2003), pp. 2947–2960.
- [5] B. W. CONNORS AND Y. AMITAI, *Generation of epileptiform discharges by local circuits in neocortex*, *Epilepsy: Models, Mechanisms and Concepts*, (1993), pp. 388–424.
- [6] S. COOMBES, G. J. LORD, AND M. R. OWEN, *Waves and bumps in neuronal networks with axo-dendritic synaptic interactions*, *Phys. D*, 178 (2003), pp. 219–241.
- [7] S. COOMBES AND M. R. OWEN, *Evans Functions for Integral Neural Field Equations with Heaviside Firing Rate Function*, *SIAM J. Appl. Dyn. Syst.*, 3 (2004), pp. 574–600.

- [8] S. COOMBES AND H. SCHMIDT, *Neural fields with sigmoidal firing rates: approximate solutions*, Discrete Contin. Dyn. Syst. Ser. S, (2010).
- [9] R. J. DOUGLAS AND K. A. MARTIN, *Neuronal circuits of the neocortex*, Annu. Rev. Neurosci., 27 (2004), pp. 419–451.
- [10] A. ELVIN, C. LAING, R. MCLACHLAN, AND M. ROBERTS, *Exploiting the hamiltonian structure of a neural field model*, Phys. D, 239 (2010), pp. 537–546.
- [11] B. ERMENTROUT, *Neural networks as spatio-temporal pattern-forming systems*, Rep. Progr. Phys., 61 (1998), pp. 353–430.
- [12] G. B. ERMENTROUT AND J. B. MCLEOD, *Existence and uniqueness of travelling waves for a neural network*, Proc. Roy. Soc. Edinburgh Sect. A, 123A (1993), pp. 461–478.
- [13] G. B. ERMENTROUT AND D. H. TERMAN, *Mathematical foundations of neuroscience*, vol. 35, Springer Science & Business Media, 2010.
- [14] J. W. EVANS, *Nerve axon equations: I linear approximations*, Indiana Univ. Math. J., 21 (1972), pp. 877–885.
- [15] ———, *Nerve axon equations: II stability at rest*, Indiana Univ. Math. J., 22 (1972), pp. 75–90.
- [16] ———, *Nerve axon equations: III stability of the nerve impulse*, Indiana Univ. Math. J., 22 (1972), pp. 577–593.
- [17] ———, *Nerve axon equations: IV the stable and the unstable impulse*, Indiana Univ. Math. J., 24 (1975), pp. 1169–1190.
- [18] G. FAYE, *Existence and Stability of Traveling Pulses in a Neural Field Equation with Synaptic Depression*, SIAM J. Appl. Dyn. Syst., 12 (2013), pp. 2032–2067.
- [19] G. FAYE AND A. SCHEEL, *Existence of pulses in excitable media with nonlocal coupling*, Adv. Math., 270 (2015), pp. 400–456.
- [20] W. GERSTNER, *Time structure of the activity in neural network models*, Phys. Rev. E, 51 (1995), p. 738.
- [21] C. D. GILBERT AND T. N. WIESEL, *Columnar specificity of intrinsic horizontal and corticocortical connections in cat visual cortex*, J. Neurosci., 9 (1989), pp. 2432–2442.
- [22] D. GOLOMB AND Y. AMITAI, *Propagating neuronal discharges in neocortical slices: computational and experimental study*, J. Neurophysiol, 78 (1997), pp. 1199–1211.
- [23] Y. GUO, *Existence and stability of traveling fronts in a lateral inhibition neural network*, SIAM J. Appl. Dyn. Syst., 11 (2012), pp. 1543–1582.
- [24] B. S. GUTKIN, G. BARD ERMENTROUT, AND J. O’SULLIVAN, *Layer 3 patchy recurrent excitatory connections may determine the spatial organization of sustained activity in the primate prefrontal cortex*, Neurocomputing, 32-33 (2000), pp. 391–400.
- [25] A. L. HODGKIN AND A. F. HUXLEY, *A quantitative description of membrane current and its application to conduction and excitation in nerve*, J. Physiol, 117 (1952), pp. 500–544.
- [26] E. M. IZHIKEVICH AND R. FITZHUGH, *Fitzhugh-nagumo model*, Scholarpedia, 1 (2006), p. 1349.
- [27] C. JONES AND N. KOPELL, *Tracking invariant manifolds with differential forms in singularly perturbed systems*, J. Differential Equations, 108 (1994), pp. 64–88.

- [28] C. K. JONES, *Stability of the travelling wave solution of the fitzhugh-nagumo system*, Trans. Amer. Math. Soc., 286 (1984), pp. 431–469.
- [29] C. K. R. T. JONES, T. J. KAPER, AND N. KOPELL, *Tracking invariant manifolds up to exponentially small errors*, SIAM J. Math. Anal., 27 (1996), pp. 558–577.
- [30] C. R. LAING AND W. C. TROY, *PDE Methods for Nonlocal Models*, SIAM J. Appl. Dyn. Syst., 2 (2003), pp. 487–516.
- [31] C. R. LAING AND W. C. TROY, *Two-bump solutions of Amari-type models of neuronal pattern formation*, Phys. D, 178 (2003), pp. 190–218.
- [32] C. R. LAING, W. C. TROY, B. GUTKIN, AND G. B. ERMENTROUT, *Multiple bumps in a neuronal model of working memory*, SIAM J. Appl. Math., 63 (2002), pp. 62–97.
- [33] J. W. LANCE, *Current concepts of migraine pathogenesis.*, Neurology, 43 (1993), pp. S11–5.
- [34] S.-H. LEE, R. BLAKE, AND D. J. HEEGER, *Traveling waves of activity in primary visual cortex during binocular rivalry*, Nat. Neurosci, 8 (2005), pp. 22–23.
- [35] J. B. LEVITT, D. A. LEWIS, T. YOSHIOKA, AND J. S. LUND, *Topography of pyramidal neuron intrinsic connections in macaque monkey prefrontal cortex (areas 9 and 46)*, J. Comp. Neurol, 338 (1993), pp. 360–376.
- [36] S. LOWEL AND W. SINGER, *Selection of intrinsic horizontal connections in the visual cortex by correlated neuronal activity*, Science, 255 (1992), pp. 209–212.
- [37] J. S. LUND, T. YOSHIOKA, AND J. B. LEVITT, *Comparison of intrinsic connectivity in different areas of macaque monkey cerebral cortex*, Cereb. Cortex, 3 (1993), pp. 148–162.
- [38] G. LV AND M. WANG, *Traveling waves of some integral-differential equations arising from neuronal networks with oscillatory kernels*, J. Math. Anal., 370 (2010), pp. 82–100.
- [39] K. A. C. MARTIN, S. ROTH, AND E. S. RUSCH, *A biological blueprint for the axons of superficial layer pyramidal cells in cat primary visual cortex*, Brain Struct. Func, 0 (2017), pp. 1–24.
- [40] D. S. MELCHITZKY, S. R. SESACK, M. L. PUCAK, AND D. A. LEWIS, *Synaptic targets of pyramidal neurons providing intrinsic horizontal connections in monkey prefrontal cortex*, J. Comp. Neurol, 390 (1998), pp. 211–224.
- [41] B. PAKKENBERG, D. PELVIG, L. MARNER, M. J. BUNDGAARD, H. J. G. GUNDERSEN, J. R. NYENGAARD, AND L. REGEUR, *Aging and the human neocortex*, Exp. Geront., 38 (2003), pp. 95–99.
- [42] D. J. PINTO AND G. B. ERMENTROUT, *Spatially structured activity in synaptically coupled neuronal networks: I. traveling fronts and pulses*, SIAM J. Appl. Math., 62 (2001), pp. 206–225.
- [43] D. J. PINTO, R. K. JACKSON, AND C. E. WAYNE, *Existence and stability of traveling pulses in a continuous neuronal network*, SIAM J. Appl. Dyn. Syst., 4 (2005), pp. 954–984.
- [44] B. SANDSTEDTE, *Evans functions and nonlinear stability of traveling waves in neuronal network models*, Int. J. Bifurc. Chaos, 17 (2007), pp. 2693–2704.
- [45] T. K. SATO, I. NAUHAUS, AND M. CARANDINI, *Traveling Waves in Visual Cortex*, Neuron, 75 (2012), pp. 218–229.

- [46] R. TRAUB, J. JEFFERYS, AND R. MILES, *Analysis of the propagation of disinhibition-induced after-discharges along the guinea-pig hippocampal slice in vitro.*, J. Physiol, 472 (1993), pp. 267–287.
- [47] H. R. WILSON AND J. D. COWAN, *Excitatory and inhibitory interactions in localized populations of model neurons.*, Biophys. J., 12 (1972), pp. 1–24.
- [48] L. ZHANG, *On stability of traveling wave solutions in synaptically coupled neuronal networks*, Differential Integral Equations, 16 (2003), pp. 513–536.
- [49] ———, *How do synaptic coupling and spatial temporal delay influence traveling waves in nonlinear nonlocal neuronal networks?*, SIAM J. Appl. Dyn. Syst., 6 (2007), pp. 597–644.
- [50] L. ZHANG, *Existence and uniqueness of wave fronts in neuronal network with nonlocal post-synaptic axonal and delayed nonlocal feedback connections*, Adv. Difference Equ., vol. 2013, article 243 (2013), pp. 1–15.
- [51] L. ZHANG AND A. HUTT, *Traveling wave solutions of nonlinear scalar integral differential equations arising from synaptically coupled neuronal networks*, Journal of Applied Analysis and Computation, 4 (2014), pp. 1–68.
- [52] L. ZHANG, L. ZHANG, J. YUAN, AND C. KHALIQUE, *Existence of wave front solutions of an integral differential equation in nonlinear nonlocal neuronal network*, in Abstr. Appl. Anal., vol. 2014, Hindawi Publishing Corporation, 2014.